Energy 205 (2020) 118058

Contents lists available at ScienceDirect

Energy

journal homepage: www.elsevier.com/locate/energy

Influence of injection scheme on flame characteristics in partially premixed combustion

Zhao Shilong [a], Fan Yuxin [a, *], Tiantai Deng [b], Danny Crookes [b]

[a] College of Energy and Power, Nanjing University of Aeronautics and Astronautics, Nanjing, 210016, China
[b] School of Electrical and Electronic Engineering and Computer Science, Queen's University Belfast, Belfast, BT7 1NN, UK

ARTICLE INFO

Article history:
Received 25 January 2019
Received in revised form
13 May 2020
Accepted 3 June 2020
Available online 9 June 2020

Keywords:
Injection scheme
Integrated stabilizer
Partial premixed combustion
Enhanced image processing method
Fuel distribution
Flame expansion

ABSTRACT

A remodelled flame holding device was integrated with injection, which could meet the demand of compact design and better resisting thermal ablation. Simplified model was applied to simulate flow field using CFD and was well verified, and the deviation was within 3%. The optimized stabilizer with close-coupled injection was put forward, its fuel distribution and flame expansion were improved with the growth of velocity. And the greater turbulent intensity was beneficial for droplets breakup and fuel/air mixing. Additionally, the growth of temperature enlarged flame expansion due to its bigger reaction rates. To more specifically illustrate combustion characteristics, an enhanced image processing method through removing flame radiation was developed to detect real flame boundary. Quantitative analysis of flame expansion was investigated to reveal the working mechanism of integrated scheme. Moreover, the influences of injection locations including prepositive and postpositive injection on flame expansion were investigated and the prepositive injection achieve up to 10% larger flame expansion. Integrated scheme was extremely important for next generation of propulsion and power system.

1. Introduction

A high-performance combustor is needed to meet the requirements of flame stabilization and propagation in a wide operation range, flame-holding systems including flame-holding device, and injection scheme are commonly used to ignite and maintain stable and reliable combustion process[1,2]. A large number of researches on flame-holding devices have been investigated, such as steps[3], cavities[4,5], struts[6], and pylons[7], etc. The working mechanism of flame-holding devices is same to form low-speed recirculation zone, steps and cavities are as pilot burner to achieve successful ignition, and struts and pylons are as radial stabilizer to conduce to flame propagation and expansion. In addition, various injection strategies are essential to achieve high-efficiency combustion process. For example, two-phase jets injected from orifice ejector[8] were experimentally investigated, and it presented that this injection scheme enhanced fluid mixing, reaction and mass transfer rates.

Injection strategies determine various combustion modes, namely, premixed combustion, non-premixed combustion and partially premixed combustion. In premixed combustion, fuel is well atomized and mixed before ignition, which is beneficial for improving combustion efficiency. For example, injectors are mounted forwardly in sequential combustor, with fuel injection into vitiated hot gas[9]. With the current trends towards higher turbine discharge temperature and requirement for satisfactory operation over extended fuel/air ratios, flame-holding device integrated with injection is expectative to operate under severe conditions of temperature and pressure to meet the requirements of next generation gas turbine engines[10].

The integration of injection scheme and flame-holding device has various combinations and works differently, due to its inherent mechanism. Fuel injection via port holes or ramps locates at combustor walls, often with additional cavities to ensure flame stabilization and favourable ignition conditions[11]. Also, bluff body is a typical configuration with a central fuel jet passing through its centre. Its flow structures, reaction zone, and dynamics of unstable flames are analysed[12,13]. Moreover, both gaseous and liquid fuel are injected into crossflow, the droplets breakup and combustion characteristics have been studied primarily. High-speed images of the flame were recorded for each operating condition and fuel injection configuration in which time-averaged chemiluminescence imaging was performed. This was done in

* Corresponding author.
E-mail address: fanyuxin@nuaa.edu.cn (F. Yuxin).

https://doi.org/10.1016/j.energy.2020.118058
0360-5442/

order to determine the dependence of the von Kármán-associated heat release oscillation amplitudes upon the mode of fuel injection and overall equivalence ratio[14,15]. For any integration, a main target is to achieve a complete and high-efficiency combustion while at the same time to minimize the length of combustor[16]. The basic principle of the flame-holding systems is to form a low speed zone for fuel/air mixing and flame stabilization[17]. In this process how to achieve flame stabilization and obtained the partially premixed flame characteristics were key issues. On the one side, a remodelled bluff body which is integrated with injection, and injectors are mounted on the sidewall of the remodelled stabilizer and the fuel is injected into the cross flow. It aimed at minimizing the length of combustor and improving resisting thermal ablation, at the same time enhancing droplets breakup and enlarging flame expansion in a short distance. The integrated scheme was a compact design to meet these demands. The performances of this remodelled stabilizer were investigated in this work, such as fuel distribution and flame expansion. On the other side, to gain extended details on working characteristics of the integrated scheme, visualization methods have been historically an invaluable diagnostic in fluid mechanics and combustion, since information on spatial distribution of the relevant variables (even just as qualitative patterns) can be most helpful to describe, or even understand, important features of a flow or a flame. Alternatively, flame images can be interpreted into a signature of a particular combustion state[18, 19]. For example, Two-colour techniques are applied to reduce sensitivity to uncertainties in emissivity or attenuation[20, 21]. The change of flame expansion angle upon the mode of overall equivalence ratio was processed using threshold method[22]. Nevertheless, the current study on flame boundary is performed roughly, for example, it doesn't tell the exact flame boundary due to the influence of radiation. An enhanced image processing method with radiation removal model is put forward, which eliminated the influence of radiation. Fuel distribution and flame spreading of this integrated scheme were captured by high-speed camera and processed using the enhanced image processing method. Quantitative analysis of fuel distribution and flame characteristics was investigated to reveal its working mechanism.

Partially premixed combustion is a complicated issue but extremely critical process. To better understand its thermal characteristics, this work is mainly focused on fuel distribution and flame propagation in the integrated stabilizer that is a combined design of injector and flame holder. The flame expansion is related with combustion efficiency, which is affected greatly by temperature and velocity. The location of close-coupled injection is key factor that needs to optimize. And in this work, the changes of fuel distribution and flame spreading are investigated using enhanced image processing method to achieve quantitative analysis. It was of great importance for advanced burner because of its compact design and resisting thermal ablation. Moreover, it was also a basic research to know the integrated scheme well, and its optimization could be performed next.

2. Methodology

In this section, flow field images was captured using Particle Image Velocimetry (PIV), which was also a method to validate numerical simulation. Images of fuel distribution and flame spreading were recorded by high-speed camera and processed automatically through an enhanced image processing method using MatLab.

2.1. Experimental set-up

A set-up for experimental study on integrated stabilizers with injectors was presented in Fig. 1. It was comprised of air supply system, fuel supply system, preheating system including combustor 1 and combustor 2, and a burner with integrated stabilizers. To ensure the same injection pressure, mass flow rate of fuel was controlled by injection pressure stabilizing valves before fuel was injected into vitiate hot gas. Thermocouples and flue gas analyser were used to monitor temperature and components of hot gas and hot gas was input into the burner. The inlet conditions of burner covered a large range, such as inlet temperatures (450–900 K) and inlet velocities (50–200 m/s). Here stated, in order to control the inlet velocity, it could be operated through regulating inlet mass flow rate that was observed and measured by vortex shedding flow meter.

The stabilizer integrated with injection was a compact design and desperately needed for the new generation of power device. The inlet conditions including velocity and temperature are greater and greater, this integrated scheme could avoid thermal ablation of injectors and auto-ignition of injected fuel. Thus, the stabilizer with close-coupled injection was put forward to solve these problems. Integrated stabilizer involved fuel injection and flame stability, and it included three geometric widths (W), such as 15 mm, 20 mm, and 30 mm. Four prepositive nozzles or postpositive nozzles were mounted on the sidewall of the stabilizers. Kerosene was injected into crossflow, additionally, the prepositive and the postpositive worked respectively. The only difference of these two injectors was location, once the prepositive injection was on, and the post positive injection was off; and vice versa. The shear force arose from large velocity gradient of recirculation zone was beneficial for droplets breakup, which was good for flame development.

In order to investigate the performances of an integrated flame holding device, such as flow field, fuel distribution and flame expansion, a rectangular burner with three kinds of integrated stabilizers was used in the experiments. The burner comprised a cross-section with a horizontal length of 100 mm and a vertical length of 120 mm as well as sidewalls made of quartz windows shown in Fig. 2, allowing full optical access for PIV and high-speed camera.

2.2. Measurement system

Particle Image Velocimetry (PIV) is an advanced technique to measure time-averaged flow fields. PIV system used in this study mainly consisted of 4 parts: Dual power 30-15 laser, a CMOS camera, a control unity and a computer. TiO_2 was used as seeding particles, of which the average diameter was 0.3 μm and density was 3800 kg/m^3. The laser beams were produced across a cylindrical lens, and focused on the plane of the reactor's vertical symmetry axis. Then, the CMOS camera, which was placed perpendicular to the laser sheet, took 30 images with 14 Hz-frequency of recording for each experimental run[23]. The images were analysed and calculated using the software package "Dynamic Studio" software, described in detail in Dantec Dynamics[24], and Tecplot to produce flow fields. According to its operating principles, flow field was calculated automatically by Dynamic Studio which brought advanced visualization capacities. And then Tecplot was used to streamline the flow pattern to present details better. And high-speed camera used for fuel distribution and flame expansion images in this experiment surpasses high definition with a 4.0 megapixel sensor capable of 730 fps at full resolution, which is applied to record the time evolutions of flame expansion with reduced vertical resolution at a rate of 1000 frames/s.

2.3. Post image processing method

The flame images captured by high speed camera were

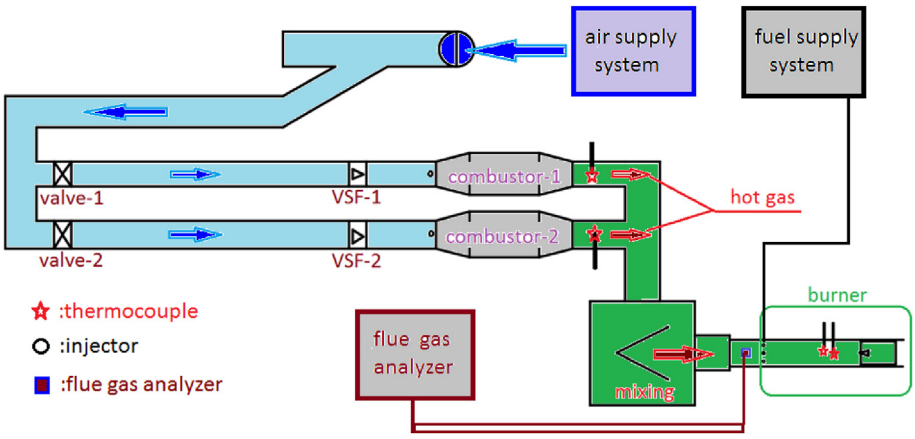

Fig. 1. Structure of experimental system.

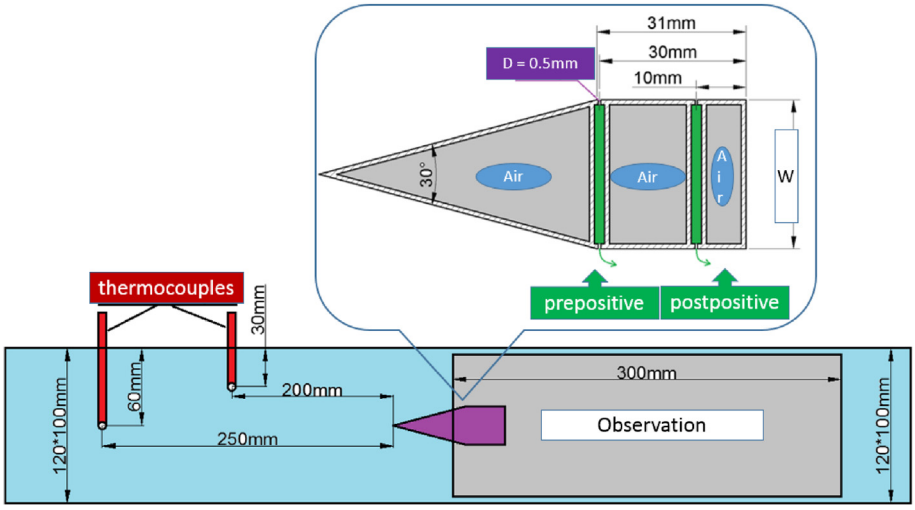

Fig. 2. Rectangular burner and enlarged stabilizer.

processed automatically through a program written in MatLab, and an enhanced image processing method was developed. Flow chart in Fig. 3 illustrated original image processing method (pathway 1) and enhanced image processing method (pathway 2). The pathways of 1 and 2 were parallel processing steps. The added model of removal radiation following pathway 2 eliminated the influence of fuzzy boundary. By the end of processing, the real flame boundary was obtained using this enhanced image processing method.

2.3.1. Original processing method: Pathway 1

The flame images captured by high-speed camera were processed to extract flame boundary. The image presented in Fig. 4 was original one captured by high-speed camera. Several filtering operators were used as pre-processing, such as dilation, erosion and Gaussian blur. Then a gradient-based operator calculated the gradient map of the image. At last, Otsu adaptive threshold transferred the flame image as a binary for further processing

Dilation (Equation (1)) eliminated the little black holes caused by flame noise. And dilation was a convolution-based image filtering using the kernel with all 'OR' in it. The specific approach was shown in Fig .5.

$$(f \oplus b)(x) = sup_{y \epsilon E}[f(y) + b(x-y)] \quad (1)$$

Erosion (Equation (2)) was used to keep the precision of the original image. Erosion was the opposite operator with 'AND' from dilation. The detailed processing step was similar to dilation.

$$(f \ominus b)(x) = inf_{y \epsilon E}[f(x+y) + b(y)] \quad (2)$$

Next, Sobel operator calculated the gradient map of the whole image. The Sobel operator was a two-stage convolution-based operation to calculate the gradient both in horizontally and vertically. The kernel of convolution was shown in Fig. 6.

According to the gradient map, Otsu adaptive threshold was applied to depict flame boundary through Otsu algorithm that was a standard and well-recognised method for distinguishing the background and flame.

2.3.2. Enhanced method: Pathway 2

Normally, the influence of flame radiation obstructed the extraction of real flame boundary. The traditional method was hard to distinguish the luminous difference between flame and radiation. As known, the grey level of top and bottom part in Fig. 4 should be 0 ideally, if there was no radiation. However, the grey level of these two parts were 15–30 because of radiation. Here assumed that the extra light intensity of top and bottom part was caused by flame entirely and the location of flame affected the two

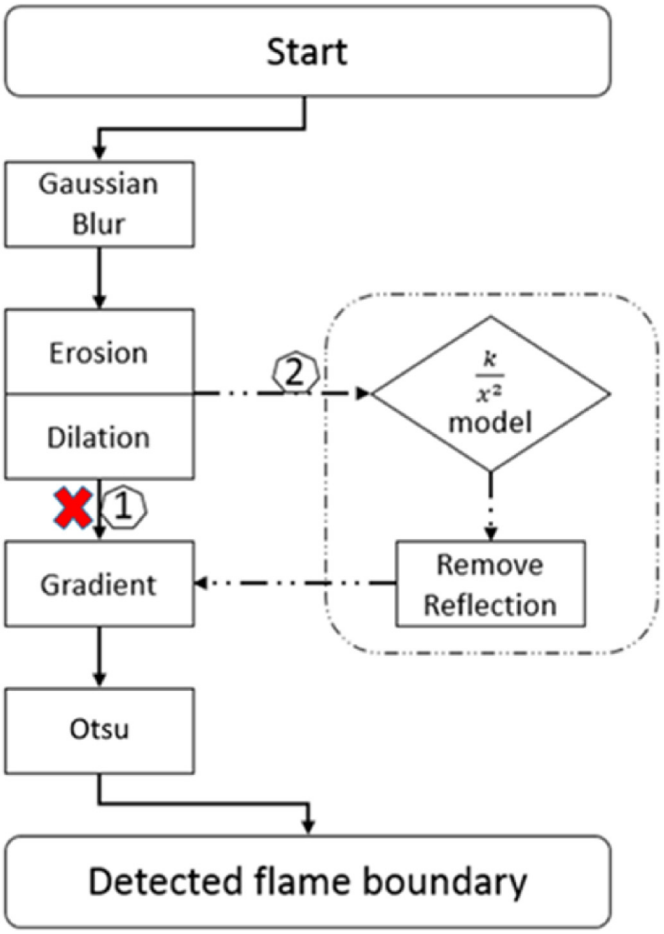

Fig. 3. Flow chart of image processing method.

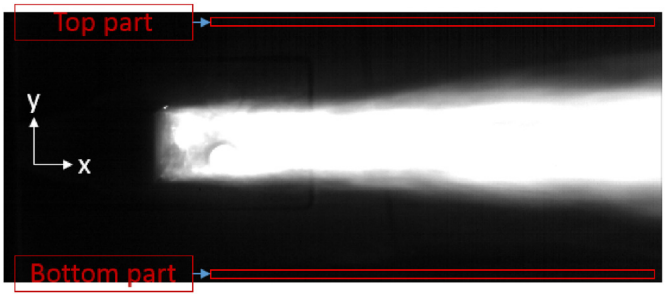

Fig. 4. Original image captured by high-speed camera.

parts differently. Due to the case the removal model was put forward to eliminate the variational radiation. According to Equation (3), where light intensity E_n represented the grey level, R was the distance between luminous location and reflected location, I_θ was the calculated value.

$$E_n = \frac{I_\theta}{R^2} \tag{3}$$

This enhanced method carried out matrixing process for the original image. Two-dimensional function was applied to present graphical information, for example, the luminous function of original image was $F(x,y)$, radiation function was $R(x,y)$, and luminous function without radiation removal was $G(x,y)$, relations of the three were shown in Equation (4) and Equation (5).

$$F(x,y) = G(x,y) + R(x,y) \tag{4}$$

$$R(x,y) = \sum_{i=0}^{n} \frac{I_\theta}{(x_i - x_0)^2 + (y_i - y_0)^2} \tag{5}$$

After removing the influence of radiation, the gradient of $G(x,y)$ was also calculated by Sobel operator and Otsu algorithm to detect real flame boundary shown in Fig .7, the brightest line was flame boundary. Compared the difference between the original and the enhanced, Fig. 8 presented the difference between original processing and enhanced image processing method.

Expansion height (in Fig. 7) was calculated, here expansion ratio at the same location behind stabilizer was defined as Equation (6):

$$\text{expansion ratio} = \frac{\textit{expansion height}}{\textit{stabilizer width}} \tag{6}$$

It was beneficial for quantitative and contrasting analysis of flame expansion, especially for various stabilizer widths.

2.4. Numerical simulation method

In the CFD model, the realizable k-e turbulent model is selected. This is due to its robustness and ability to fit the initial iteration, design lectotype and parametric investigation. The near wall was processed using a standard wall function method. Pressure and velocity coupling is achieved using the SIMPLE (Semi-Implicit Method for Pressure Linked Equations) algorithm. The meshes around stabilizer were refined, where the minimum is 0.3 mm and the maximum is 0.5 mm. Also, it was compared with smaller size (0.2mm−0.3 mm) and bigger size (0.5mm−0.7 mm) of meshes to verify mesh independence. The results showed mesh size had little influence on the numerical simulation. Numerical method was used to simulate flow field in the burner and simulation model was of the same geometric size with experimental structure shown schematically in Fig. 2 (left-inlet, right-outlet). The detailed

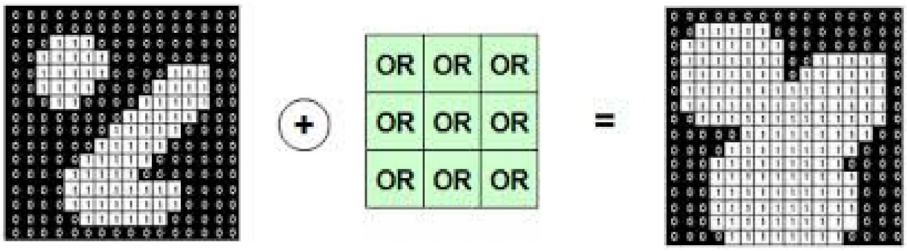

Fig. 5. Dilation processing for the original image.

$$\frac{\partial}{\partial x} = \begin{bmatrix} -1 & 0 & 1 \\ -2 & 0 & 2 \\ -1 & 0 & 1 \end{bmatrix} \qquad \frac{\partial}{\partial y} = \begin{bmatrix} -1 & -2 & -1 \\ 0 & 0 & 0 \\ 1 & 2 & 1 \end{bmatrix}$$

Fig. 6. Multi-dimensional gradient calculation using Sobel operator.

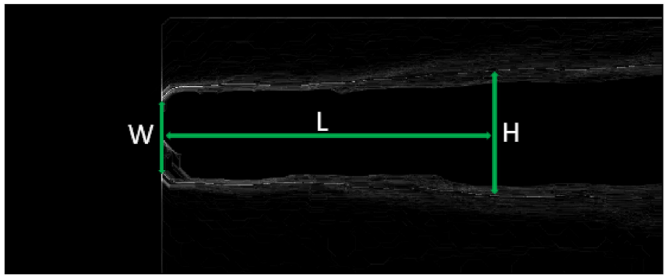

Fig. 7. The detected flame boundary (stabilizer width: W, distance from stabilizer: L, expansion height: H).

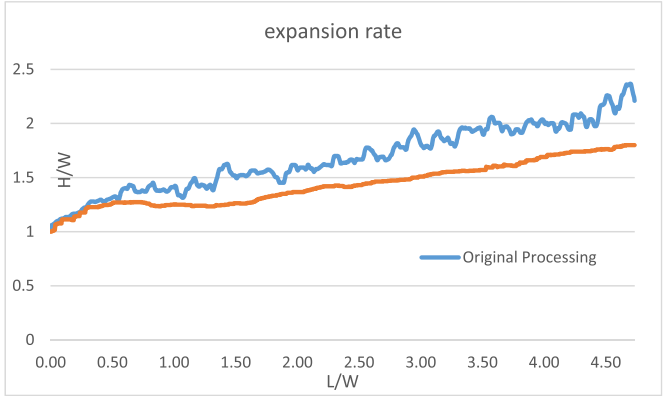

Fig. 8. The change of flame expansion rate using two image processing methods.

boundary conditions are shown in Table 1 [25].

3. Results and discussion

In the following section, remodelled stabilizer was investigated on flow filed, fuel distribution and flame structure. The characteristics of partially premixed combustion was extremely important for integrated stabilizer design.

3.1. Flow field and numerical validation

Fig. 9 showed the time-averaged vector fields coupled with streamlines measured by PIV for various widths of stabilizers at 50 m/s and 320 K inlet conditions. It illustrated the effect of widths on the development of eddies after bluff body. With the decrease of width, asymmetric pair eddies were broken into unsteady single-eddy appeared firstly, and then eddy disappeared. The decrease and disappearance of vortex shortened the fuel residence time and induced unsteady combustion. Based on the experimental data, the primary lectotype of stabilizer width was conducted. Cold flow field of 30 mm-width stabilizer which produced couple-vorticity recirculation was simulated and validated by experimental data.

The comparison of Fig. 10 and Fig. 9 presented the pair eddies formed after 30 mm-width stabilizer were validated at 50 m/s. The vertical dash lines in Figs. 9 and 10 were the cut-off lines, the length ratios of recirculation zone and stabilizer width were measured and calculated by MATLAB. It was through calculating the lattices of matrix. The deviation of recirculation zone was within 3%. Good agreement was observed between the numerical and experimental results. Therefore, the numerical method employed in this investigation can be used for further simulation of flow field to analyse aerodynamic characteristics. As shown in Fig. 10, pair eddies that always existed and located within1.5-width axial distance behind stabilizer were asymmetric with the growing velocity. Flow field presented fluctuation and wavy contours of velocity were related to axial location of the asymmetric eddies. Also, the fluctuation of recirculation zone had a greater promotion of droplets breakup and fuel/air mixing.

As to partially premixed combustion, the capacity of mixing was correlated closely with combustion performance. Turbulent kinetic energy was an index to evaluate turbulence that reinforced heat and mass transfer directly. As shown in Fig. 11, it were turbulent kinetic energy contours at 50 m/s and 100 m/s. As shown there was a big difference of turbulent intensity behind the stabilizer due to different velocities. At a higher velocity, the turbulent intensity and pulse amplitude were greater and stronger, it was beneficial for promoting fuel/air mixing.

3.2. The change of fuel distribution and flame spreading

Flame characteristics were the key issues to evaluate the integrated scheme, and the atomization and diffusion of fuel were intermediate processes that are influenced flow field and affect flame spreading directly. The detailed and in-depth investigation on the change of fuel distribution and flame spreading was extremely important.

Table 1
Boundary conditions.

Boundary conditions	Boundary location	Parameters
Velocity inlet	Inlet	V = 50, 100, 150, 200 m/s; T = 320 K
Outflow	Outlet	
Wall	Solid wall and liquid boundary	Stationary wall; no slip; no heat flux

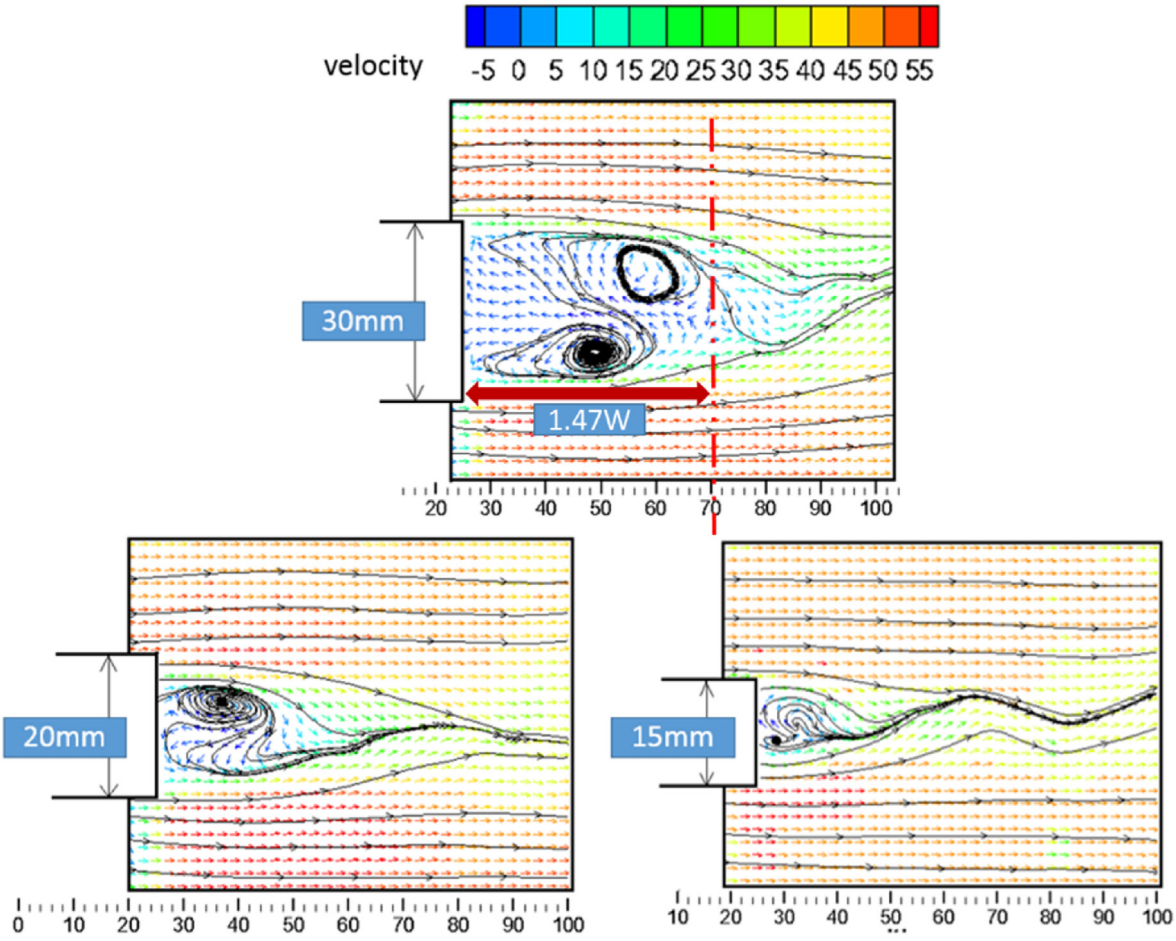

Fig. 9. Flow field measured by PIV at 50 m/s and 320 K

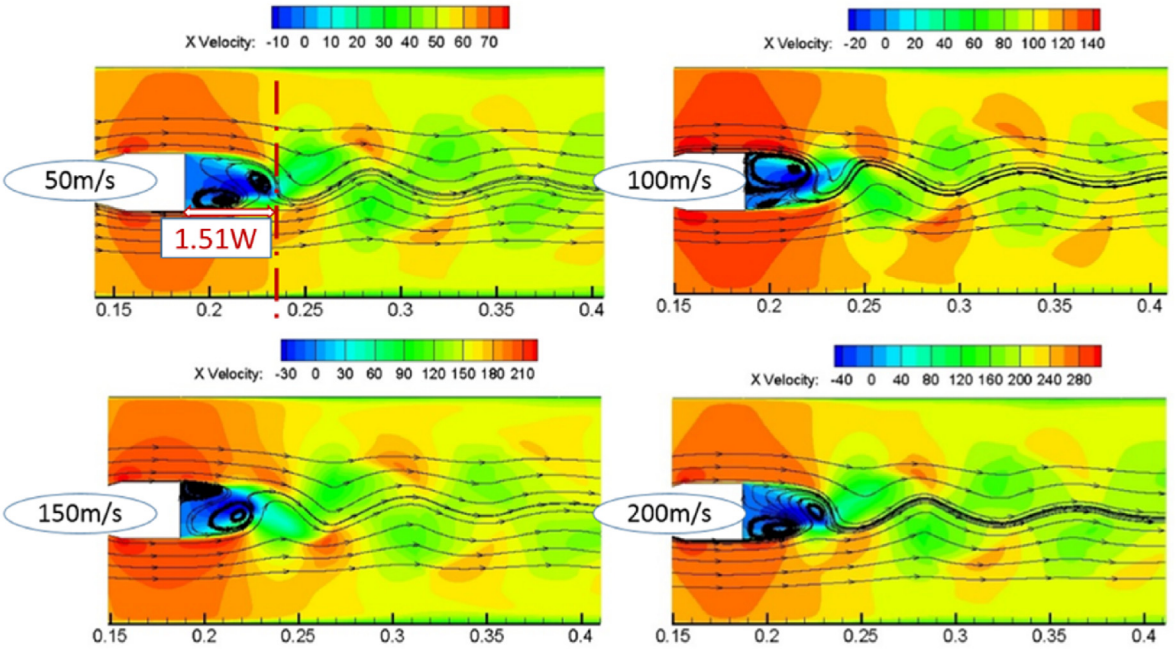

Fig. 10. Numerical simulation for 30 mm-width stabilizer at various velocities.

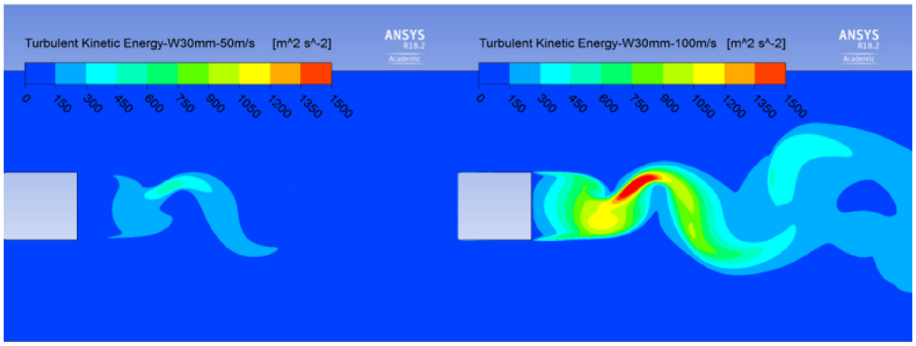

Fig. 11. Turbulent Kinetic Energy contours at 50 m/s and 100 m/s.

Fuel distribution was measured by high speed camera and light sheet, and 30 mm-width and prepositive-injectors stabilizer was tested at 50 m/s and 100 m/s. In Fig. 12, it was showed images of fuel distribution at different momentum ratios of injection, where momentum ratio of injection was defined as the ratio of injection momentum and main flow momentum. At the same inlet velocity, the growing momentum ratios of injection can't improve mixing capacity of fuel/air, because penetration depth was greater, which led injected fuel away from shear layer of the recirculation zone. The entrainment ability of recirculation zone was hard to take fuel into zone directly behind stabilizer. Thus, increasing momentum ratios of injection led to thinner fuel distribution in the recirculation zone.

The growth of velocity affected the fuel distribution greatly. It was due to the increase of velocity gradient and turbulent intensity arose from the growth of velocity, which strengthen the capacity of shear force and mass transfer. Thus, it was good for droplets breakup and fuel/air mixing. Moreover injected fuel was attached on the sidewall and was taken into shear layer at a higher velocity, droplet breakup was promoted then it followed with gas movement and was entrained into recirculation zone. The turbulent intensity of recirculation zone was strong and extensive at a higher velocity, it was good for fuel/air mixing and diffusion.

The cases of Fig. 12(a) and (d) were ignited and captured by high speed camera. These two cases were kept with same fuel/air ratio shown in Fig. 13. The marked oval circle were hollowed-out flame that was due to its little fuel mixing and diffusion, and hollowed-out area of flame at 100 m/s was much smaller. Moreover, at a lower velocity (at a smaller turbulence intensity), flame lied on different layers, which led to non-uniform outlet temperature. Rather, at a higher velocity (at a larger turbulent intensity), fierce combustion occurred around the recirculation zone then expanded backward. As to integrated stabilizer, the distribution of fuel and flame was greatly affected by velocity, namely, turbulent intensity. Great turbulent intensity reinforced not only flame distribution but also diffusion.

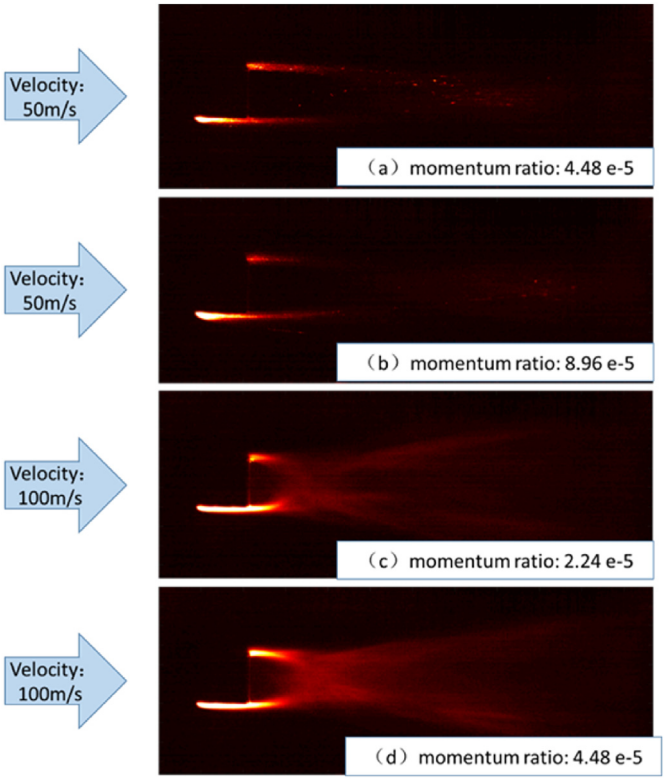

Fig. 12. Comparison of fuel distribution at different momentum ratios of injection.

3.3. Influence of injectors location on flame expansion

Injectors were mounted on the sidewall of stabilizer, and its location affected fuel distribution even combustion performance. To better investigate the influence of injection location, such as prepositive and postpositive nozzle, quantitative analysis was performed using the enhanced image processing method mentioned in 2.3. Also, 30 mm-width stabilizer was as the experimental model.

Fig. 14 showed the change of expansion ratio at various velocities and temperatures. As presented, the influence of injectors location on flame expansion was obvious, expansion ratio of the prepositive was greater than it of the postpositive at the same

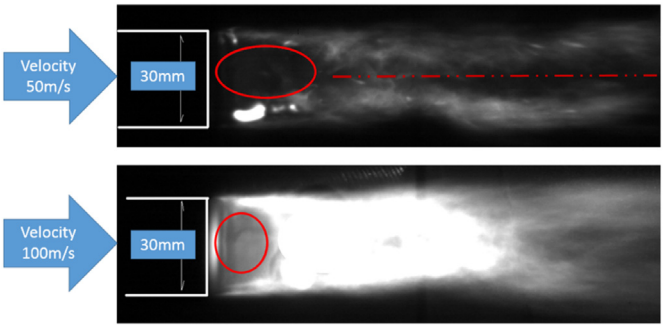

Fig. 13. Comparison of flame spreading at 50 m/s and 100 m/s.

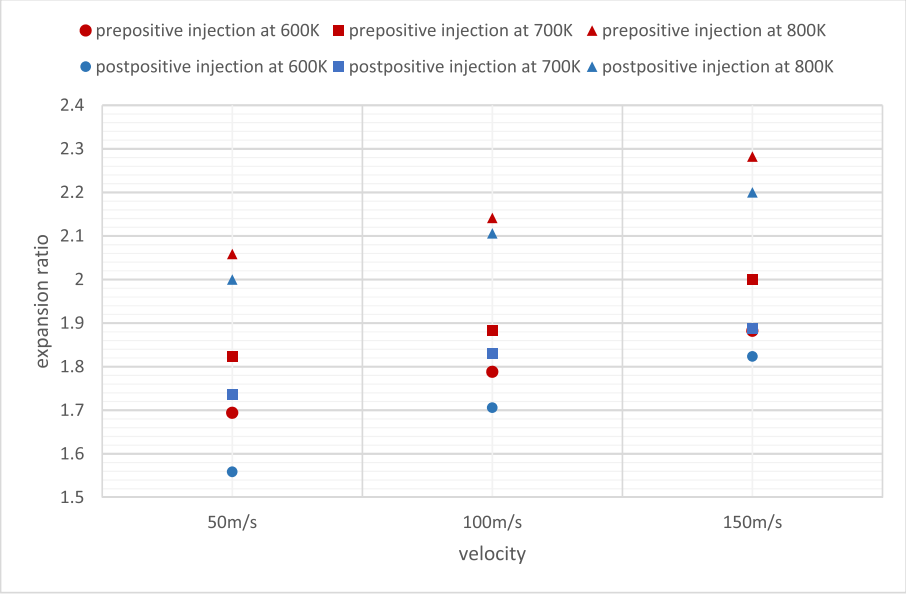

Fig. 14. Change of flame expansion ratio at various velocities and temperatures.

velocity and temperature. The reason was that the friction and collision between fuel and sidewall of stabilizer enhanced droplets breakup and diffusion to prepositive injection. It provided a better fuel distribution and was beneficial to flame spreading.

The growth of velocity and temperature promoted flame spreading. On the one side, the greater turbulent intensity arose from growing velocity strengthened heat and mass transfer, thus it accelerated flame spreading and extended flame expansion. On the other side, the growth of temperature improved the evaporation of droplets and reaction rate, which increased local equivalent ratio and intensified the reaction processes; the overall combustion was an endothermic process, the growth of temperature could reduce the energy barriers and accelerate the occurrence of combustion.

4. Conclusions

In this work, analysis of partially premixed combustion in an integrated stabilizer was investigated detailedly. Numerical and experimental study on flow field was conducted, and fuel distribution and flame spreading were tested and captured. An enhanced image processing was as a helper method to digitize flame expansion.

(1) An enhanced image processing method was developed to remove radiation that caused the extra 20% light intensity, this flame image processing method eliminated the influence of dizzy boundary. Furthermore, it was applied to calculate flame expansion height specifically.
(2) Simplified model of CFD was used to simulate flow field and was well verified, and the deviation was within 3%. Fuel distribution of an optimized integration scheme was investigated via experimental study. It showed higher turbulent intensity arose from higher velocity enhanced droplets breakup, diffusion and distribution in downstream recirculation zone of integrated scheme, and reinforced flame diffusion to expand flame distribution area.
(3) Injector locations, such as prepositive and postpositive injection, had extremely obvious and important impact on flame expansion. Quantitative analysis presented flame expansion of the prepositive injection was greater up to 10%. Additionally, higher inlet velocity and temperature also enhanced the flame expansion.

Declaration of competing interest

We declare that we do not have any commercial or associative interest that represents a conflict of interest in connection with the work submitted.

CRediT authorship contribution statement

Zhao Shilong: Conceptualization, Methodology, Software, Writing - original draft. **Fan Yuxin:** Validation, Formal analysis, Writing - review & editing. **Tiantai Deng:** Methodology, Software. **Danny Crookes:** Writing - review & editing.

Appendix A. Supplementary data

Supplementary data to this article can be found online at https://doi.org/10.1016/j.energy.2020.118058.

References

[1] Lovett J, Brogan T, Philippona D, Kiel B, Thompson T. July). Development needs for advanced afterburner designs. In: 40th AIAA/ASME/SAE/ASEE joint propulsion conference and exhibit; 2004. p. 4192.
[2] Markstein GH, editorvol. 75. Elsevier; 2014. Nonsteady flame propagation: AGARDograph.
[3] Cheng TS, Yang WJ. Numerical simulation of three-dimensional turbulent separated and reattaching flows using a modified turbulence model. Comput Fluid 2008;37(3):194–206.
[4] Zhang RC, Bai NJ, Fan WJ, Yan WH, Hao F, Yin CM. Flow field and combustion characteristics of integrated combustion mode using cavity with low flow resistance for gas turbine engines. Energy 2018;165:979–96.
[5] Hassanvand A, Gerdroodbary MB, Fallah K, Moradi R. Effect of dual micro fuel jets on mixing performance of hydrogen in cavity flameholder at supersonic flow. Int J Hydrogen Energy 2018;43(20):9829–37.
[6] Choubey G, Pandey KM. Effect of different wall injection schemes on the flowfield of hydrogen fuelled strut-based scramjet combustor. Acta Astronaut 2018;145:93–104.
[7] Freeborn AB, King PI, Gruber MR. Swept-leading-edge pylon effects on a scramjet pylon-cavity flameholder flowfield. J Propul Power 2009;25(3):571–82.
[8] Park SK, Yang HC. An experimental investigation of the flow and mass transfer

behavior in a vertical aeration process with orifice ejector. Energy 2018;160:954–64.
[9] Schulz O, Noiray N. Autoignition flame dynamics in sequential combustors. Combust Flame 2018;192:86–100.
[10] Shivakumar DK, Sabbani G, Singh G, Revanasiddappa PH. Prediction of gas turbine afterburner performance using CFD for different operating conditions and reheat strength. In: ASME 2017 gas turbine India conference. American Society of Mechanical Engineers; 2017, December. V001T04A004-V001T04A004.
[11] Laurence S, Martinez Schramm J, Karl S, Hannemann K. April). An experimental investigation of steady and unsteady combustion phenomena in the HyShot II combustor. In: 17th AIAA international space planes and hypersonic systems and technologies conference; 2011. p. 2310.
[12] Zhang RC, Fan WJ, Xing F, Song SW, Shi Q, Tian GH, Tan WL. Experimental study of slight temperature rise combustion in trapped vortex combustors for gas turbines. Energy 2015;93:1535–47.
[13] Zhang R, Xu Q, Fan W. Effect of swirl field on the fuel concentration distribution and combustion characteristics in gas turbine combustor with cavity. Energy 2018;162:83–98.
[14] Cross C, Lubarsky E, Shcherbik D, Bonner K, Klusmeyer A, Zinn BT, Lovett JA. January). Determination of equivalence ratio and oscillatory heat release distributions in non-premixed bluff body-stabilized flames using chemiluminescence imaging. In: ASME 2011 turbo expo: turbine technical conference and exposition. American Society of Mechanical Engineers; 2011. p. 549–58.
[15] Cross C, Fricker A, Shcherbik D, Lubarsky E, Zinn BT, Lovett JA. Dynamics of non-premixed bluff body-stabilized flames in heated air flow. In: ASME turbo expo 2010: power for land, sea, and air. American Society of Mechanical Engineers; 2010, October. p. 875–84.
[16] Förster FJ, Dröske NC, Bühler MN, von Wolfersdorf J, Weigand B. Analysis of flame characteristics in a scramjet combustor with staged fuel injection using common path focusing schlieren and flame visualization. Combust Flame 2016;168:204–15.
[17] Zhang J, Chang J, Shi W, Hou W, Bao W. Combustion stabilizations in a liquid kerosene fueled supersonic combustor equipped with an integrated pilot strut. Aero Sci Technol 2018;77:83–91.
[18] Hernandez R, Ballester J. Flame imaging as a diagnostic tool for industrial combustion. Combust Flame 2008;155(3):509–28.
[19] Kohse-Höinghaus K, Barlow RS, Aldén M, Wolfrum J. Combustion at the focus: laser diagnostics and control. Proc Combust Inst 2005;30(1):89–123.
[20] Shimoda M, Sugano A, Kimura T, Watanabe Y, Ishiyama K. Prediction method of unburnt carbon for coal fired utility boiler using image processing technique of combustion flame. IEEE Trans Energy Convers 1990;5(4):640–5.
[21] Lu G, Gilabert G, Yan Y. Vision based monitoring and characterisation of combustion flames. J Phys Conf 2005;15(1):194. IOP Publishing.
[22] Zhao S, Yuxin F, Xiaolei Z. Influence of parameters on flame expansion in a high-speed flow: experimental and numerical study. Proc IME J Power Energy 2019:0957650919896504.
[23] Du H, Shi Z, Cheng K, Li G, Lu J, Li Z, Hu L. The study of flow separation control by a nanosecond pulse discharge actuator. Exp Therm Fluid Sci 2016;74:110–21.
[24] Dynamic Studio software and introduction to PIV instrumentation. Dantec Dynamics GmbH; 2000. Publication number: 9040U3625.
[25] Zhao S, Fan Y. Experimental and numerical study on thermodynamic performance in a designate pilot-ignition structure: Step. Aero Sci Technol 2019;91:561–70.